

# Sunitinib-Induced Cardiotoxicity Is Mediated by Off-Target Inhibition of AMP-Activated Protein Kinase

Risto Kerkela<sup>1</sup>, Kathleen C. Woulfe<sup>1,2</sup>, Jean-Bernard Durand<sup>4</sup>, Ronald Vagnozzi<sup>1,2</sup>, David Kramer<sup>5</sup>, Tammy F. Chu<sup>6,7</sup>, Cara Beahm<sup>1</sup>, Ming Hui Chen<sup>6,7</sup>, and Thomas Force<sup>1,2,3</sup>

## Abstract

Tyrosine kinase inhibitors (TKIs) are transforming the treatment of patients with malignancies. One such agent, sunitinib (Sutent, Pfizer, New York, NY, USA), has demonstrated activity against a variety of solid tumors. Sunitinib is “multitargeted,” inhibiting growth factor receptors that regulate both tumor angiogenesis and tumor cell survival. However, cardiac dysfunction has been associated with its use. Identification of the target of sunitinib-associated cardiac dysfunction could guide future drug design to reduce toxicity while preserving anticancer activity. Herein we identify severe mitochondrial structural abnormalities in the heart of a patient with sunitinib-induced heart failure. In cultured cardiomyocytes, sunitinib induces loss of mitochondrial membrane potential and energy rundown. Despite the latter, 5' adenosine monophosphate-activated protein kinase (AMPK) activity, which should be increased in the setting of energy compromise, is reduced in hearts of sunitinib-treated mice and cardiomyocytes in culture, and this is due to direct inhibition of AMPK by sunitinib. Critically, we find that adenovirus-mediated gene transfer of an activated mutant of AMPK reduces sunitinib-induced cell death. Our findings suggest AMPK inhibition plays a central role in sunitinib cardiomyocyte toxicity, highlighting the potential of off-target effects of TKIs contributing to cardiotoxicity. While multitargeting can enhance tumor cell killing, this must be balanced against the potential increased risk of cardiac dysfunction.

**Keywords:** AMPK, cancer therapeutics

## Introduction

Sunitinib is a multitargeted tyrosine kinase inhibitor (TKI) that prolongs survival in patients with renal cell carcinoma and gastrointestinal stromal tumors (GIST) and has demonstrated single agent activity against a number of other solid tumors.<sup>1–3</sup> In addition, approximately 200 active clinical trials involving thousands of patients are currently registered (www.clinicaltrials.gov). However, cardiac dysfunction can be associated with the agent, with 8–15% of patients developing congestive heart failure (CHF) and others developing asymptomatic left ventricular systolic dysfunction.<sup>4,5</sup> Furthermore, we found that apoptosis was induced by sunitinib in cardiomyocytes in culture and in the mouse heart *in vivo*. However, the specific mechanisms regulating this injury (i.e., the molecular target of sunitinib, inhibition of which induces the toxicity) are not known. As demonstrated by Fernandez et al., identification of this target(s) would potentially allow redesign of sunitinib to avoid the target responsible for cardiotoxicity while leaving tumor cell killing intact.<sup>6,7</sup>

Sunitinib is one of two approved multitargeted agents, the other being sorafenib (Nexavar, Onyx/Bayer, Leverkusen, Germany). Sunitinib inhibits a number of growth factor receptors regulating both tumor cell proliferation/survival and tumor angiogenesis, including vascular endothelial growth factor receptors (VEGFRs) 1–3, platelet-derived growth factor receptors (PDGFRs)  $\alpha$  and  $\beta$ , c-Kit, FLT3, CSF1R, and RET.<sup>8–10</sup> We thought it likely that inhibition of one of these might account for the cardiotoxicity; however, of the known targets of sunitinib, only VEGFRs and PDGFRs are expressed in the heart. VEGFRs are expressed in endothelial cells of the coronary vasculature, where at least in experimental models they play an important role in the heart by maintaining the vasculature in the setting of stress induced by excessive pressure load.<sup>11</sup> We have previously demonstrated substantial hypertension in patients treated with sunitinib.<sup>4</sup> Thus, sunitinib-mediated inhibition of VEGFRs could contribute to the

observed cardiac dysfunction in patients. However, since VEGFRs are not expressed in cardiomyocytes, sunitinib-mediated VEGFR inhibition would not account for the direct toxicity we observed when isolated cardiomyocytes are exposed to sunitinib.<sup>4</sup>

PDGFRs, which are expressed in cardiomyocytes, have been reported to serve a protective role in the heart exposed to ischemic injury.<sup>12,13</sup> However, these studies employed exogenous administration of PDGF to the heart, and it is unclear if inhibition of endogenous PDGFRs, as one would see with sunitinib, would induce cardiotoxicity. Therefore, we asked whether inhibition of kinases not known to be targets of sunitinib might account for the toxicity.

Guided by findings on transmission electron microscopy (TEM) of an endomyocardial biopsy of a patient with sunitinib-associated heart failure, we identified striking mitochondrial abnormalities, suggesting energy compromise might contribute significantly to the LV dysfunction seen with this agent. Herein we present data suggesting that off-target inhibition by sunitinib of AMPK, a kinase that plays key roles in maintaining metabolic homeostasis in the heart, especially in the setting of energy stress, accounts, at least in part, for the toxicity seen in cardiomyocytes exposed to sunitinib. This, therefore, represents the first example of off-target inhibition of a kinase by a TKI leading to cardiotoxicity. Importantly, follow-up biopsy of the patient one month after discontinuing drug showed striking resolution of the mitochondrial injury, suggesting the potential of significant reversibility at the ultrastructural level.

## Methods

### Materials

Sunitinib capsules were purchased from a pharmacy. AICAR was from BioMol International (Plymouth Meeting, PA, USA),

<sup>1</sup>Center for Translational Medicine; <sup>2</sup>Program in Cell and Developmental Biology; <sup>3</sup>Cardiology Division, Thomas Jefferson University, Philadelphia, PA, USA; <sup>4</sup>Department of Cardiology, M.D. Anderson Cancer Center, Baylor College of Medicine, Houston, TX, USA; <sup>5</sup>South Texas Pathology, San Antonio, TX, USA; <sup>6</sup>Department of Cardiology, Children's Hospital Boston, Boston, MA, USA; <sup>7</sup>Department of Medicine, Divisions of Women's Health and Gender Biology, and Cardiovascular Medicine, Brigham and Women's Hospital, Harvard Medical School, Boston, MA, USA.

Correspondence: T Force (thomas.force@jefferson.edu)

DOI: 10.1111/j.1752-8062.2008.00090.x

and Compound C was from Calbiochem (Darmstadt, Germany). Antibodies employed were as follows: Akt; phospho-Ser 473 Akt; phospho-Ser 112 Bad; phospho-Ser 155 Bad; phospho-Thr 172 AMPK; phospho-Thr 56 eEF2; and phospho-Ser 79 ACC-1 (which recognizes both ACC-1 and ACC-2 isoforms when phosphorylated) were from Cell Signaling (Beverly, MA, USA). Isolectin B4 antibody was from Vector Laboratories (Burlingame, CA, USA), GAPDH antibody from R&D Systems (Minneapolis, MN, USA), and antibody against vinculin (which along with GAPDH functioned as the loading control) was from Sigma-Aldrich (St. Louis, MO, USA). Antibody against phospho-Ser 136 Bad was from Calbiochem and phospho-Tyr 705 STAT3 antibody was from Upstate Biotechnology, Inc (Billerica, MA, USA).

### Animal studies

C57Bl/6 mice were fed sunitinib mixed with chow (25 mg/kg/day) for 5 weeks. Determination of cardiomyocyte cross-sectional area on hematoxylin and eosin-stained sections was done as previously described.<sup>14</sup> For determination of capillary density, the primary antibody to Isolectin B4 was added in blocking solution (2% BSA, 0.2% horse serum in PBS supplemented with 0.2% NP-40) and incubated overnight. Vectastin Elite ABC kit (Vector Laboratories) and DAB Plus Kit (Zymed Laboratories, Carlsbad, CA, USA) were used as instructed by the manufacturers. Spot Imaging software (Diagnostic Instruments, Inc., Sterling Heights, MI, USA) was used to record images. For determination of capillary density, capillaries were counted by an observer blinded to the treatment conditions. At least three areas per section were counted, and at least three sections per heart were examined.

Animal protocols were approved by the Institutional Animal Care and Use Committee of Thomas Jefferson University.

### Cell culture

Neonatal rat ventricular myocytes (NRVMs) were isolated from 2- to 3-day old Sprague-Dawley rats (Charles River Laboratories, Wilmington, MA, USA) as previously described.<sup>7</sup> For experiments, contents of the sunitinib capsules were solubilized in distilled water, and insoluble material was removed by repeated centrifugation at 2,500 g, prior to addition to the cells for the times and at the concentrations noted in the figures and legends.

### Adenovirus-mediated gene transfer

NRVMs were transduced with the adenovirus encoding AMPK $\alpha$ -1(1–312) or with an adenovirus encoding green fluorescent protein as a control, at a multiplicity of infection of 25 for 24 hours prior to performing experiments.

### Immunoblotting and densitometry

Immunoblotting and densitometry determinations were performed as described<sup>7</sup> using an Odyssey Infrared Imaging System (LI-COR, Lincoln, Nebraska, USA). Vinculin or GAPDH were used as a loading control.

Visualization of apoptotic cells by terminal deoxynucleotidyl transferase-mediated dUTP nick end labeling (TUNEL; kit from Chemicon International, Billerica, MA, USA) was performed following the manufacturer's instructions. Apoptotic cells were visualized with a Nikon Eclipse 80i microscope and software from NIS-elements was used to record images. Studies to examine mitochondrial membrane potential ( $\Delta\Psi_m$ ) employed Mito-Tracker Green (Invitrogen, Carlsbad, CA, USA) and were performed as previously described.<sup>7</sup>

### Quantification of [ATP]

ATP concentration was determined with a kit from Calbiochem, following the manufacturer's instructions.

### Determination of IC<sub>50</sub> for sunitinib versus various kinases

Inhibitory concentration 50 (IC<sub>50</sub>) is the concentration of inhibitor (i.e., sunitinib) that inhibits activity of a kinase by 50%. Three different biochemical kinase assay formats were employed to determine IC<sub>50</sub> values for sunitinib versus the various kinases. Briefly, for all experiments, recombinant human full-length or GST-kinase domain fusion proteins were utilized in the assays. IC<sub>50</sub> measurements of compound versus kinases were based on autophosphorylation or phosphorylation of kinase peptide substrates in the presence of ATP and divalent cation (MgCl<sub>2</sub> or MnCl<sub>2</sub> 10–20 mM). The linear range of kinase activity was determined for each kinase and all kinetic measurements, and IC<sub>50</sub> determinations were performed in this range. Standard criteria for goodness of fit were applied to accept or reject assay values for inhibition. Modifications of this included employing determination of production of ADP from ATP that accompanies phosphoryl transfer to the substrate. Importantly, three formats were used to determine IC<sub>50</sub> for sunitinib versus AMPK (Kinaxo™ (Kinaxo, Inc., Munich, Germany) and Pfizer and Pharmacia biochemical kinase assays), and there was good agreement across the assay formats, with values ranging from 0.135 to 0.38  $\mu$ M.

In a second set of assays performed by Invitrogen, which focused specifically on AMPK, the catalytic subunits ( $\alpha_1$  or  $\alpha_2$ ) were coexpressed with the regulatory subunits ( $\gamma_1$  and  $\beta_1$ ) in a baculovirus expression system. After purification of the three subunits, the purified AMPK was further activated by incubation with the upstream AMPK activator, CAMKK1. AMPK was again purified and then incubated with AMP (100  $\mu$ M) to achieve maximal activation. IC<sub>50</sub> values were then determined for sunitinib and a frequently used AMPK small molecule inhibitor, Compound C, using four formats: radiometric and three proprietary fluorescence-based assay formats (LanthaScreen™, Z'-LYTE™, and Omnia™; see <http://www.invitrogen.com/site/us/en/home/Products-and-Services/Applications/Drug-Discovery/DD-Misc/Drug-Discovery-Posters.html#kinases> for more information).

### Statistical analyses

We employed two-tailed Student's *t*-test for unpaired samples for all statistical analyses. A Bonferroni correction was employed for multiple comparisons. A *p* value of <0.05 was considered significant.

## Results

### Sunitinib induces myocyte injury *in vivo*

We (D. K.) obtained an endomyocardial biopsy in a patient with renal cell carcinoma, who developed acute decompensated systolic heart failure after 11 months of sunitinib treatment (37.5 mg daily on the FDA approved schedule of 4 weeks on treatment/2 weeks off treatment). Prior to starting sunitinib, the patient had a B-type natriuretic peptide (BNP) of 79 pg/mL (normal < 80 pg/mL) and an LVEF of 65%. When the patient presented with heart failure, BNP was 2,300 pg/mL and LVEF had decreased to 20–25%. The patient had no history of coronary artery disease, and subsequent coronary angiography showed no flow-limiting disease. Endomyocardial biopsy showed no evidence of myocarditis. However, widespread and severe structural alterations in mitochondria on TEM were found, which included markedly swollen mitochondria with disrupted or absent cristae (Figure 1).

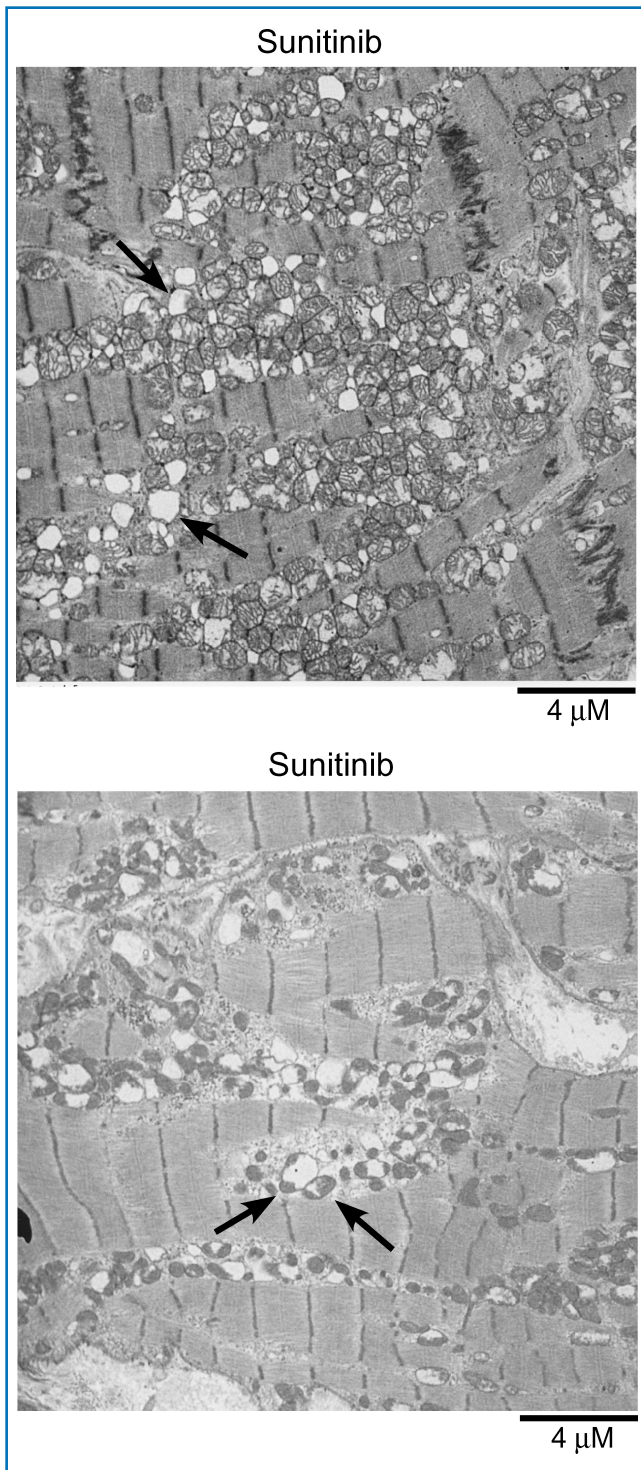


**Figure 1. Transmission electron micrographs of endomyocardial biopsies from a patient presenting with sunitinib-associated congestive heart failure.** Throughout the sections there is a range of injury from swollen mitochondria with markedly effaced cristae and disruption of normal mitochondrial architecture to large mitochondrial “ghosts,” lacking any remnants of cristae (top panel, arrows). Bottom panel shows many swollen mitochondria with a markedly swollen one (left arrow) and a moderately swollen one (right arrow) adjacent to several mitochondria that appear normal.

### Sunitinib induces apparent myocyte loss in the mouse

We had seen similar mitochondrial abnormalities in mice treated with sunitinib<sup>4</sup> and asked if this impacted LV function or remodeling in the mouse. We saw no adverse effects of sunitinib

	Vehicle	Sunitinib (5 weeks)
FS (%)	26.4 ± 1.56	31.3 ± 5.07
EF (%)	44.8 ± 2.34	52.5 ± 6.85
LVEDD (mm)	3.76 ± 0.22	3.51 ± 0.18
LVESD (mm)	2.82 ± 0.22	2.41 ± 0.27 *
LVPW (mm)	0.75 ± 0.11	0.86 ± 0.06
LVW/BW (mg/g)	4.58 ± 0.32	4.49 ± 0.28

EF = ejection fraction; FS = fractional shortening; LVEDD and LVESD = left ventricular end-diastolic and end-systolic dimensions, respectively; LVPW = left ventricular posterior wall thickness; LVW/BW = left ventricular mass normalized to body weight. Data are mean ± SD. \**p* < 0.05 versus vehicle-treated.

**Table 1.** Echocardiographic indices of sunitinib-treated mice.

on any of several echocardiographic parameters in mice treated with 25 mg/kg/day for 5 weeks (Table 1). However, although LV mass was similar in sunitinib- and vehicle-treated mice, direct measurement of cardiomyocyte size on H & E-stained heart sections showed cardiomyocyte hypertrophy in the sunitinib-treated hearts (Figure 2A). Although we did not see

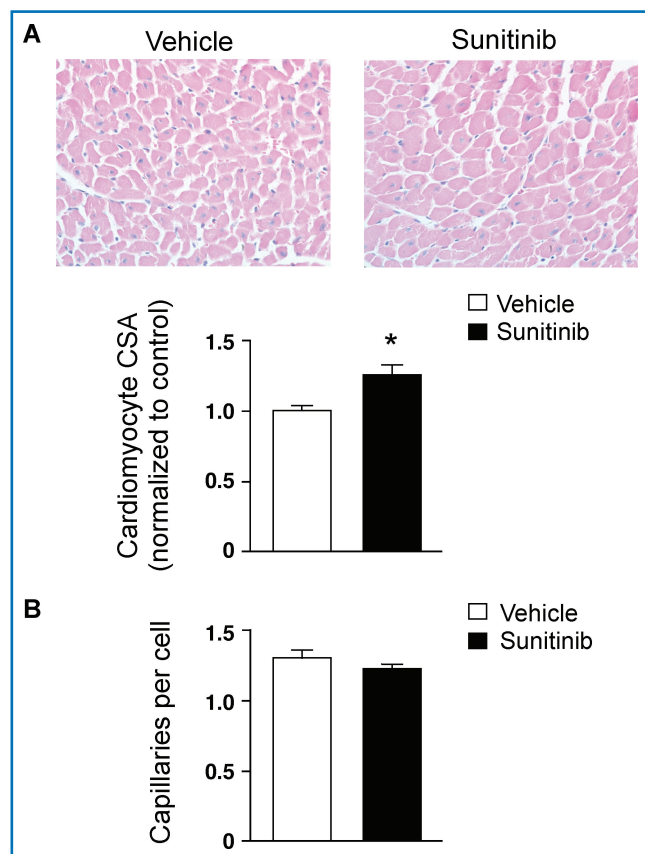


**Figure 2. Effect of sunitinib on myocardial remodeling and capillary density.**

Mice were fed sunitinib (25 mg/kg/day) or vehicle (H<sub>2</sub>O) mixed with chow for 5 weeks.<sup>15,21</sup> Heart sections were then stained with hematoxylin and eosin (A) or isolectin B4 to identify endothelial cells (B). (A) Cardiomyocyte hypertrophy in sunitinib-treated mice. Cardiomyocyte cross-sectional area (CSA) was determined by an observer blinded to the treatment conditions. Graph shows quantitation for *n* = 4 vehicle-treated and 4 sunitinib-treated mice. \**p* < 0.01 versus vehicle-treated. (B) Sunitinib does not alter myocardial capillary density. Capillary density was determined in *n* = 3 vehicle-treated and 3 sunitinib-treated hearts by an observer blinded to the treatment conditions. Capillary number is expressed relative to the number of nuclei in the fields. A similar analysis that quantified capillary number per unit area yielded similar results (data not shown).

a statistically significant increase in rates of apoptosis in these mice in the absence of additional hemodynamic stress induced by phenylephrine infusion,<sup>4</sup> cardiomyocyte hypertrophy without an accompanying increase in cardiac mass in the sunitinib-treated mice is consistent with myocyte loss. Thus, either myocytes were dying by nonapoptotic processes, key windows of increased apoptosis were missed, or the small increase in apoptosis we had previously seen in the mouse<sup>4</sup> over time was sufficient to reduce cardiomyocyte number.

#### Sunitinib does not alter capillary density

We then asked whether inhibition of VEGFRs by sunitinib had any adverse consequences on the vasculature of the heart, which might contribute to the cardiotoxicity. We found no differences in capillary density in mice treated with sunitinib for 5 weeks compared with controls, as assessed by staining for either von Willebrandt Factor (not shown) or with an antibody to isolectin B4 (Figure 2B). These findings are consistent with VEGF/VEGFRs being more important in the creation of new vessels than in the maintenance of existing vessels.<sup>15</sup> Although an effect of VEGFR inhibition on vascular function (as opposed to vessel number) cannot be excluded, the mice were not hypertensive,<sup>4</sup> suggesting eNOS function was not markedly impaired. This, together with the lack of expression of VEGFRs in cardiomyocytes, suggests inhibition of VEGFRs is not a major mechanism underlying the cardiotoxicity of sunitinib in our model.

#### Molecular mechanisms of sunitinib cardiotoxicity—dysregulation of AMPK signaling

Given the marked structural mitochondrial damage noted in the TEMs of the patient (Figure 1) and in the mice treated with sunitinib,<sup>4</sup> we asked whether sunitinib could directly lead to collapse of  $\Delta\Psi_m$  in cardiomyocytes in culture. We found significant sunitinib-induced loss of  $\Delta\Psi_m$  (Figure 3A). We also found that cardiomyocyte energetics were impaired in sunitinib-treated cardiomyocytes, since [ATP] was significantly reduced even at a relatively early time point following treatment (Figure 3B).

We then turned to protein kinase signaling pathways that are recruited in the setting of mitochondrial injury and energy compromise to see if they were dysregulated, possibly accounting for the cardiotoxicity. In the setting of energy depletion, activation of AMPK in cardiomyocytes is a protective response, which serves to restrict energy utilization and increase energy production (see Figure 7A for a schematic of AMPK signaling).<sup>16–18</sup> Surprisingly, based on determination of the  $IC_{50}$  for sunitinib versus AMPK in kinase assays *in vitro*, we found that AMPK was potentially a direct target of sunitinib, inhibiting AMPK with an  $IC_{50}$  of  $216 \pm 58$  nM ( $n = 4$  data sets; Table 2). This  $IC_{50}$  is comparable to that for the known sunitinib target, RET (224 nM).<sup>19</sup> Furthermore, we felt that this  $IC_{50}$  for AMPK could potentially be relevant *in vivo* since trough blood levels of sunitinib plus its major active metabolite in patients taking the FDA-approved dosage regimen are of the order of 125–250 nM.<sup>20–23</sup> In addition, the high volume of distribution of sunitinib (2,230 L; [http://www.pfizer.com/files/products/uspi\\_sutent.pdf](http://www.pfizer.com/files/products/uspi_sutent.pdf)) suggests tissue levels would be substantially higher than those achieved in the blood.

Further supporting the contention that AMPK is inhibited by sunitinib at biologically relevant concentrations, Invitrogen's Kinase Profiling Services employed four different assay formats to determine  $IC_{50}$  for sunitinib against AMPK that had been previously maximally activated (Methods). These studies

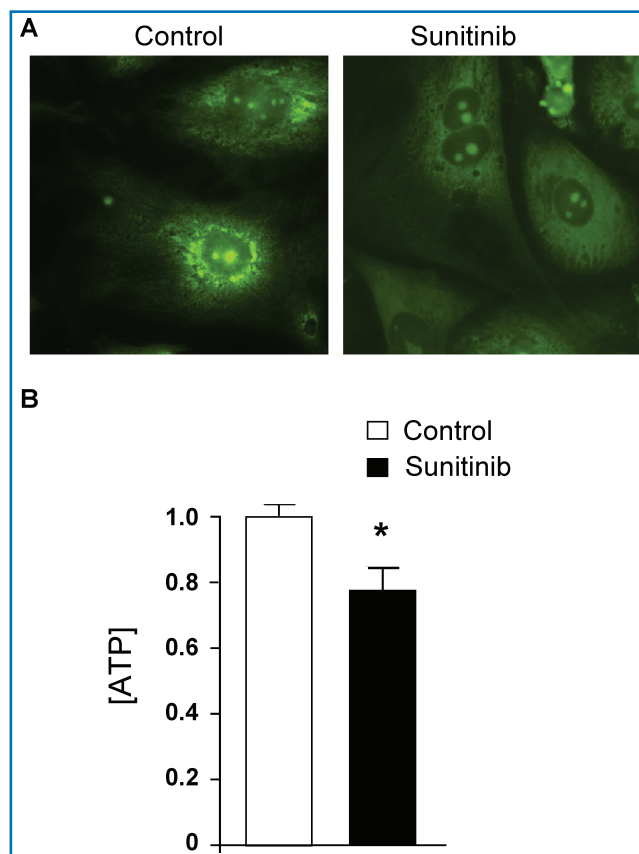


**Figure 3. Sunitinib induces loss of mitochondrial membrane potential ( $\Delta\Psi_m$ ) and reduction in [ATP]. (A)** Loss of ( $\Delta\Psi_m$ ). Cells were treated with vehicle (Control) or 1  $\mu$ M sunitinib for 12 hours and then were stained with Mito-Tracker Green. Note the punctate appearing stain in the vehicle-treated cells, consistent with mitochondrial localization, and the diffuse stain in the sunitinib-treated cells, consistent with loss of  $\Delta\Psi_m$ . These images are representative of multiple fields from five separate experiments. **(B)** [ATP] in cardiomyocytes is reduced by treatment with sunitinib. Cells were treated with vehicle (control) or sunitinib for 8 hours and then lysates were analyzed for ATP content. ATP content in the control was normalized to a value of 1. Bar graphs show average + SEM ( $n > 5$  for each group). The experiment was repeated four times. \* $p < 0.05$  versus control.

Kinase	Mean $IC_{50}$ ( $\mu$ M)
Akt1	3.8 to > 10
Akt2	> 10
Akt3	> 10
ERK1	> 10
ERK2	> 10
CAMKK1	5.25
LKB1	> 10
AMPK	0.216
mTORC1	> 10
mTORC2	> 10

Minimum number of sets of assays done for each kinase was two with a range of two to seven. Various formats of recombinant biochemical kinase assays were used (see Methods).

**Table 2.**  $IC_{50}$  values for sunitinib activity against various protein kinases.

gave markedly lower  $IC_{50}$  values for sunitinib ranging from 6.5 to 37 nM for the AMPK $\alpha_1$  subunit and 4.8 to 72 nM for the AMPK $\alpha_2$  subunit (<http://www.invitrogen.com/site/us/en/home/Products-and-Services/Applications/Drug-Discovery/DD-Misc/>

Drug-Discovery-Posters.html#Kinases). These data suggest that sunitinib is a potent inhibitor, particularly of activated AMPK. By contrast,  $IC_{50}$  values for Compound C ranged from 88 to 700 nM.

We next asked what effect sunitinib had on AMPK in cells (cultured NRVMs). Sunitinib did not alter expression levels of

AMPK (Figure S1). However, we found a modest but consistent increase in phosphorylation of AMPK at the activating site (Threonine (T)172) in NRVMs treated with sunitinib (Figure 4A). T172 is phosphorylated by kinases upstream of AMPK (CAMKKs and LKB1; see Figure 7A for schematic), and

these data suggest that neither of these kinases were inhibited by sunitinib *in situ*. Consistent with this conclusion, the  $IC_{50}$  for sunitinib versus CAMKK1 was 4.5–6  $\mu$ M and for LKB1 was >10  $\mu$ M (Table 2), values that are clearly too high to be relevant *in vivo*.

We next examined the effect of sunitinib on the ability of AMPK to phosphorylate and activate downstream targets in the cell. Kinases transfer phosphate groups from ATP to substrates, thereby altering activity of the substrate. Thus ATP binding to the kinase is essential for the kinase's activity. Sunitinib's mechanism of action is to compete with ATP for binding to the kinase, thereby preventing the transfer of phosphate to the substrate (Figure 7A). Therefore, to determine if sunitinib inhibits AMPK in the cell, one must examine whether sunitinib blocks phosphorylation of AMPK substrates. One bona fide AMPK substrate in the cell is acetyl co-A carboxylase (ACC). There are two isoforms—ACC1 and ACC2—and both are expressed in NRVMs. Phosphorylation by AMPK of ACC1 inhibits lipid biosynthesis and of ACC2 leads to increased fatty acid oxidation (thereby limiting energy depletion). We found that ACC1/2 expression was not altered by sunitinib treatment (Figure S1), but sunitinib significantly reduced phosphorylation of ACC1/2 in NRVMs (Figure 4B). In the heart *in vivo*, ACC2 is the dominant isoform and phosphorylation of ACC2 was also significantly reduced in mice treated with sunitinib (Figure 4C). Furthermore, sunitinib significantly reduced activity of AMPK following treatment with the AMPK activator, AICAR, as determined by ACC phosphorylation (Figure 4D). Thus, sunitinib inhibits AMPK activity *in vitro*, in cardiomyocytes in culture, and in the heart. Furthermore, the degree of inhibition is comparable to that seen with another AMPK inhibitor, Compound C (Figure 4D). These data suggest that the energy rundown occurring in the setting of sunitinib therapy, which might otherwise have recruited AMPK, was unable to do so due to sunitinib's direct inhibition of AMPK. This could be expected to exacerbate energy depletion and injury (Figure 7A).<sup>16–18,24</sup>

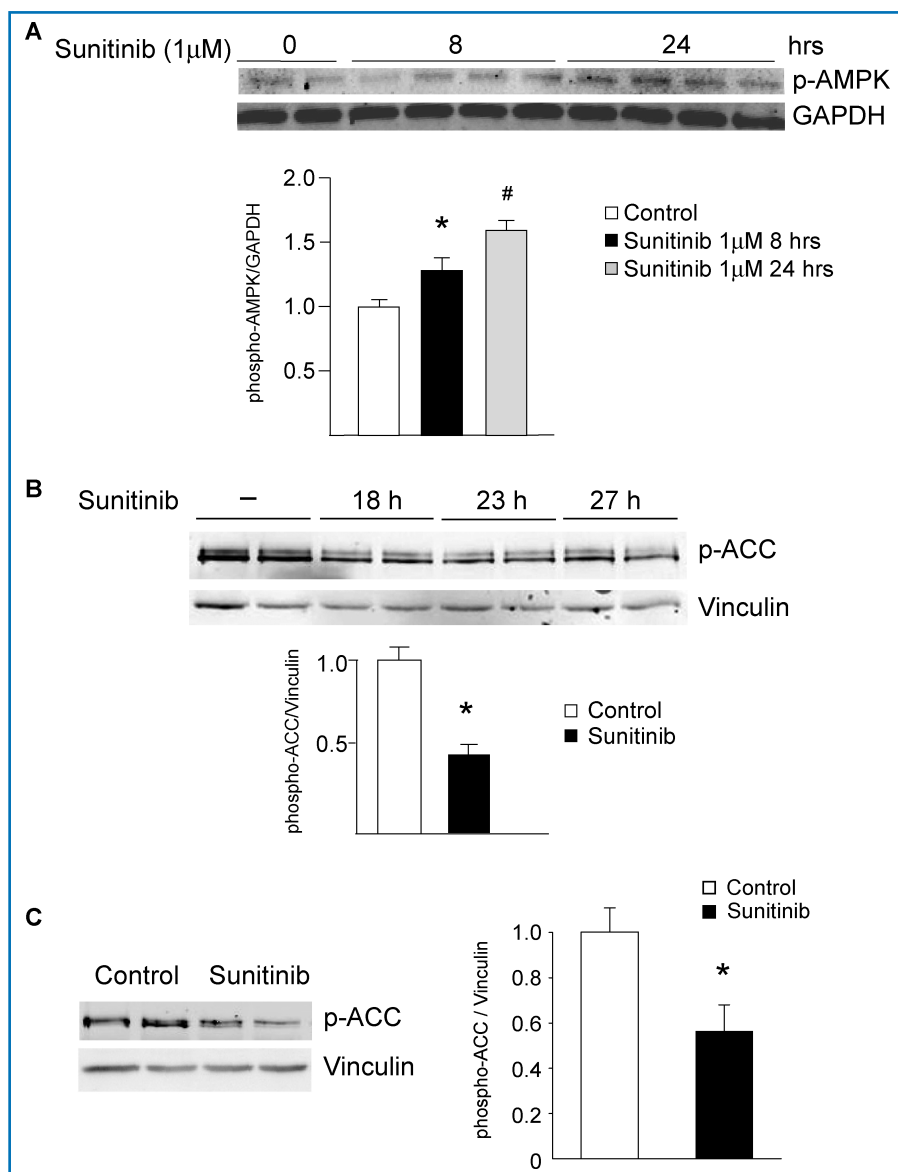


**Figure 4. Sunitinib inhibits AMPK signaling *in vitro* and *in vivo*.** (A) AMPK activation state is not inhibited by sunitinib. NRVMs were treated with sunitinib (1  $\mu$ M) for the times shown, and then lysates were immunoblotted with anti-phospho-AMPK (T172). Quantification is shown, normalized to the loading control (GAPDH). There is a statistically significant increase in activation state as determined by T172 phosphorylation.  $n = 4$ ; \* $p < 0.01$  versus control. (B) Sunitinib inhibits AMPK activity in NRVMs. NRVMs were treated with sunitinib (1  $\mu$ M) for the times shown, and then lysates were immunoblotted with anti-phospho ACC antibody. This antibody recognizes both ACC1 phosphorylated at Ser 79 and ACC2 phosphorylated at Ser 221. Quantification is shown, normalized to the loading control (vinculin).  $n = 4$ ; \* $p < 0.01$ . (C) Sunitinib inhibits AMPK activity *in vivo*. Mice were treated for 5 weeks with sunitinib (25 mg/kg/day) and then heart lysates were immunoblotted for phospho-ACC. Quantification is shown, normalized to the loading control (vinculin). \* $p < 0.05$  versus control.  $n = 4$  hearts per condition. (D) Inhibition of AICAR-induced activation of AMPK by sunitinib and by the AMPK inhibitor, Compound C. Top panel. NRVMs were pretreated with vehicle (sunitinib 0) or sunitinib at the concentrations shown for 4 hours. Cells were then treated with the AMPK activator, AICAR (1 mM) versus vehicle (–) for 1 hour. Lysates were immunoblotted with anti-phospho-ACC. Controls (lanes 1 and 2) are from the same gel as lanes 3–8. Bottom panel. NRVMs were pretreated with vehicle (–) or Compound C at the concentrations shown for 4 hours and then were treated with 1 mM AICAR versus vehicle (–) for 1 hour. Lysates were then processed as above. In both panels, quantification is shown normalized to the loading control (vinculin). Top panel,  $n = 4$ ; \* $p < 0.01$ ; \*\* $p < 0.001$ . (E) Sunitinib enhances eEF2 phosphorylation. NRVMs were treated with sunitinib (1  $\mu$ M) for the times shown. Lysates were immunoblotted with anti-phospho eEF2 antibody. Phosphorylation is normalized to the GAPDH loading control. Note the significant increase in phosphorylation of eEF2 in response to sunitinib (compare lanes 1–2 with lanes 3–10).  $n = 4$ ; \* $p < 0.01$ .

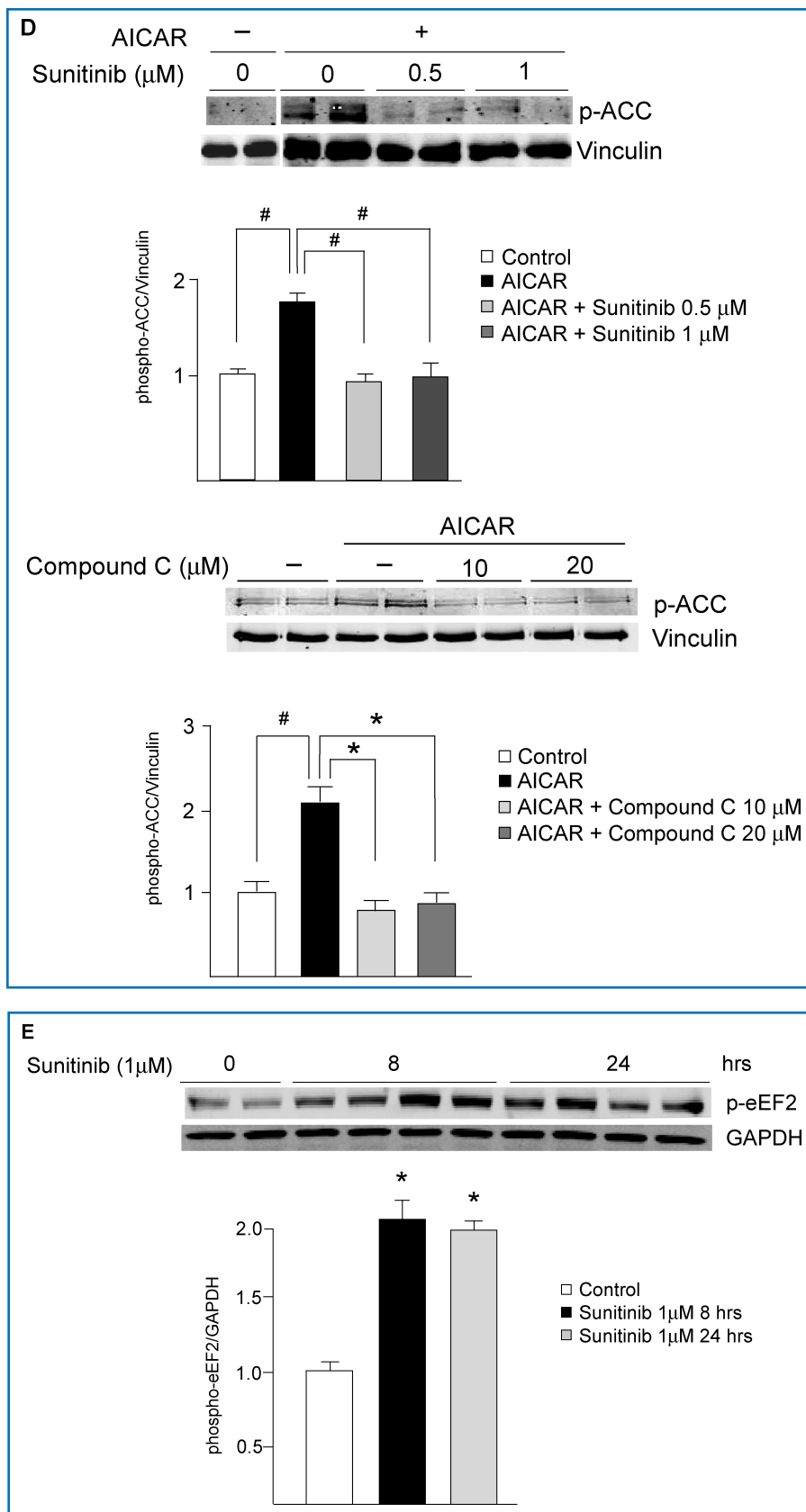


Figure 4. Continued.

**Indirect inhibition of the mTOR complex 1 (mTORC1) by sunitinib**

We also examined the activation state of the other key pathway that is regulated by alterations in energy status and cell growth conditions- mTORC1 (see Figure 7B for a schematic of mTORC1 signaling). One key target downstream from mTORC1 in the response to energy stress is the eukaryotic elongation factor 2 kinase (eEF2K) and its target, the translation elongation factor eEF2, which is a central regulator of protein synthesis.<sup>25</sup> In settings not supportive of growth (e.g., energy depletion or inhibition of signaling downstream of growth factor receptors), mTOR is inhibited, leading to eEF2K activation and phosphorylation of eEF2, blocking further protein synthesis and thereby reducing ATP utilization. mTORC1 can be inhibited by AMPK, but since AMPK was inhibited in sunitinib-treated cells, we expected that mTORC1 would not be appropriately inhibited in the setting of sunitinib treatment despite the ATP depletion. Surprisingly, we found that mTORC1 was potently inhibited in sunitinib-treated cells, as evidenced by the marked increase in phosphorylation of eEF2 in response to sunitinib in the absence of any other stimulus (Figures 4E and 7B). Thus, the marked increase in eEF2 phosphorylation is consistent with significant energy compromise induced by sunitinib and also demonstrates that mTORC1 was appropriately inhibited in this setting, in spite of the dysregulation of AMPK signaling. Importantly, this was not due to direct inhibition of mTORC1 by sunitinib since IC<sub>50</sub> for sunitinib versus mTORC1 (and mTORC2) was >10 $\mu\text{M}$  (Table 2). Thus, sunitinib inhibits AMPK but also leads to recruitment of an AMPK-independent pathway regulating mTORC1, and the latter leads to appropriate eEF2 phosphorylation and, thereby, a reduction in protein translation (Figure 7B). This is consistent with sunitinib leading to recruitment of one or more of the multiple factors in addition to AMPK that lead to mTORC1 inhibition including inhibition of growth factor receptor tyrosine kinase (RTK) signaling.<sup>26-28</sup>

**Other key prosurvival pathways in the heart are not dysregulated by sunitinib**

In the inhibitor screen, several additional tyrosine, as well as serine/threonine

kinases, were identified as potential targets of sunitinib,<sup>29</sup> but most were either not expressed in the heart or were not known to play a major role in cardiomyocyte survival. Two kinases—Janus kinase 1 (JAK1) and the Ribosomal S6 kinase (RSK) family members RSK2 and RSK3—were candidate contributors to the cardiotoxicity of sunitinib. However, we found no evidence that these putative targets were actual targets in the cell (data not shown). Furthermore, we found no evidence of sunitinib-mediated inhibition of either of two key prosurvival kinases—the ERK family or Akt family—in either *in vitro* kinase assays (Table 2) or in cells (data not shown).

#### Inhibition of AMPK accounts, at least in part, for sunitinib cardiotoxicity

Our data show that of all the pathways examined above, only AMPK was clearly dysregulated, but whether this dysregulation was contributing to the sunitinib-induced cardiomyocyte toxicity was not clear. We found that treatment of cardiomyocytes with Compound C also induced collapse of  $\Delta\Psi_m$  (Figure 5A) and reduction in [ATP] (Figure 5B). Furthermore, Compound C induced apoptosis (as determined by TUNEL staining) to a degree comparable to that induced by sunitinib (Figure 5C). Thus, an AMPK inhibitor unrelated to sunitinib was able to recapitulate the abnormalities induced by sunitinib in cardiomyocytes, suggesting (though certainly not proving) AMPK inhibition is a key mechanism of the toxicity. Furthermore, Compound C is not a selective inhibitor of AMPK. Therefore, to more definitively determine whether inhibition of AMPK played a key role in sunitinib cardiomyocyte toxicity, we employed adenovirus-mediated gene transfer of a constitutively active mutant of AMPK, AMPK $\alpha$ -1(1–312) (Figure S2). This mutant lacks the autoinhibitory sequence and can be fully activated by LKB1 or CaMKKs, without the other AMPK subunits being present. We found that AMPK $\alpha$ -1(1–312) was activated in cardiomyocytes following adenovirus-mediated gene transfer as determined by phosphorylation of T172 (Figure 6A, top panel). Consistent with this, expression of AMPK $\alpha$ -1(1–312) significantly enhanced phospho-ACC, indicative of enhanced AMPK signaling (Figure 6A, middle and bottom panels). Furthermore, even in the presence of sunitinib, AMPK $\alpha$ -1(1–312) maintained phospho-ACC at levels significantly greater than those in cells treated with sunitinib in the absence of AMPK $\alpha$ -1(1–312) (Figure 6A, middle panel, compare lanes 4–5 with lanes 6–8, and bottom panel for quantification). Most importantly, expression of AMPK $\alpha$ -1(1–312) significantly reduced sunitinib-induced cardiomyocyte death as determined by TUNEL (Figure 6B). Thus off-target inhibition of AMPK by the multitargeted TKI sunitinib appears to account, at least in part, for sunitinib-induced cardiomyocyte toxicity.

#### Sunitinib-induced mitochondrial injury appears to be largely reversible at the ultrastructural level

Follow-up biopsy of the patient described above, performed 1 month after discontinuation of sunitinib and institution of angiotensin converting enzyme inhibitor and  $\beta$ -blocker therapy, showed striking improvement with clear evidence of mitochondrial biogenesis (Figure 6C). While some mitochondrial abnormalities were still evident, these were relatively minor. Clinically, the patient improved and was able to resume sunitinib therapy, albeit at a lower dose.

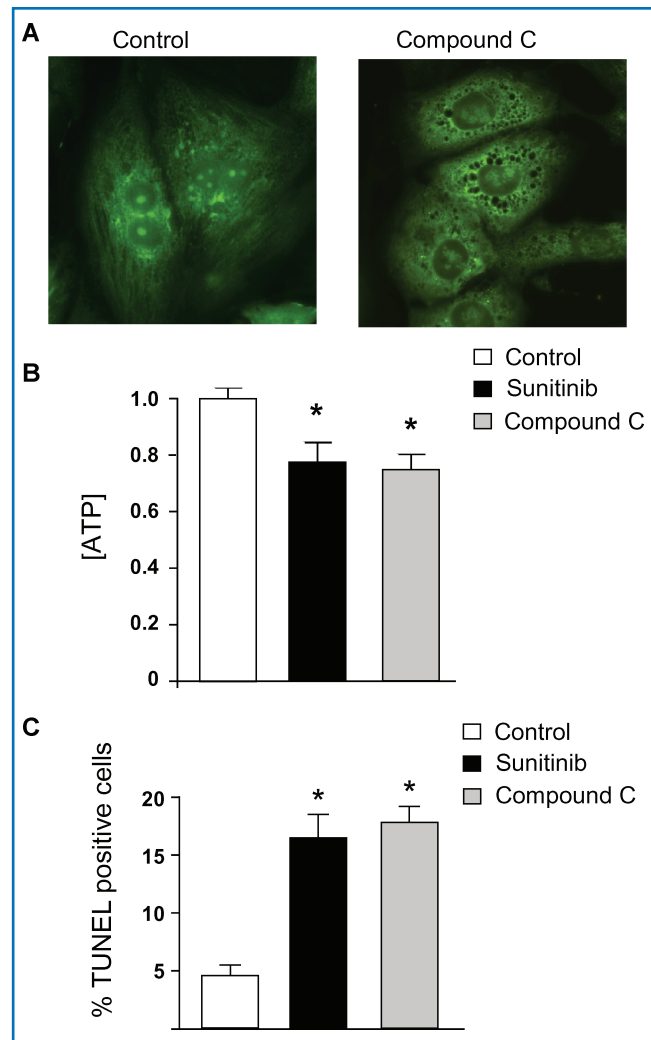
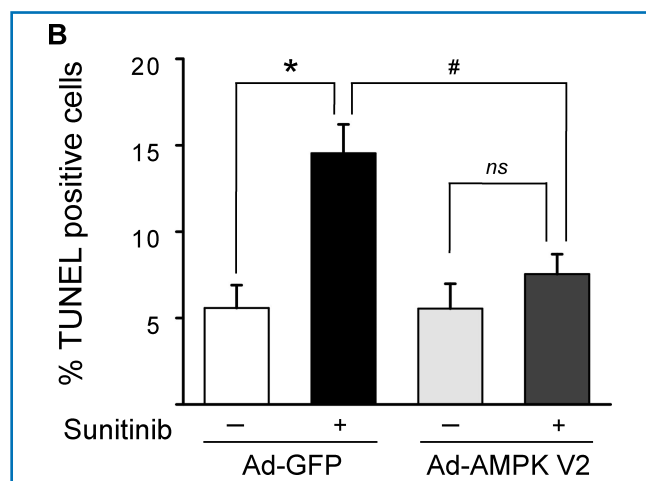
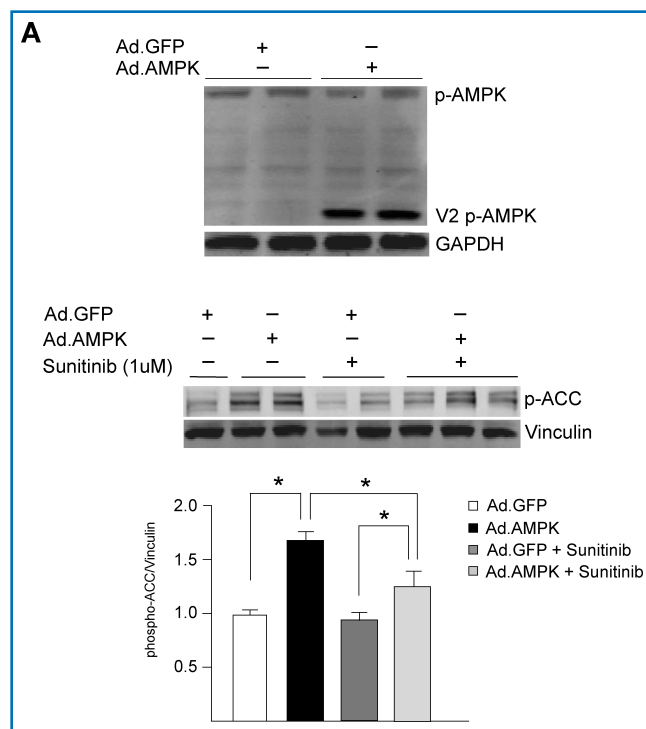


**Figure 5. A second AMPK inhibitor, Compound C, also induces collapse of  $\Delta\Psi_m$ , ATP depletion, and cell death.** (A) Compound C leads to collapse of  $\Delta\Psi_m$ . Cardiomyocytes were treated with vehicle (control) versus Compound C (10  $\mu$ M) for 12 hours and then were stained with Mito-Tracker Green. Diffuse staining in Compound C-treated cells is consistent with collapse of  $\Delta\Psi_m$ . These images are representative of multiple fields from three separate experiments and were done in parallel with those shown in Figure 3A. (B) Sunitinib and Compound C induce comparable degrees of ATP depletion. Cardiomyocytes were treated with vehicle (control), sunitinib, or Compound C for 8 hours prior to determination of ATP concentration. \* $p < 0.05$  versus control. (C) Sunitinib and Compound C induce cardiomyocyte apoptosis. Cardiomyocytes were treated with vehicle (control), sunitinib, or Compound C for 28 hours and then were fixed and stained for TUNEL. \* $p < 0.05$  versus control.

#### Discussion

Herein we demonstrate that sunitinib can lead to profound structural and functional abnormalities of mitochondria in patients and in cardiomyocytes in culture. The morphologic findings in the TEMs of the patient are consistent with opening of the mitochondrial permeability transition pore. Consistent with this, we saw collapse of  $\Delta\Psi_m$  in cultured cardiomyocytes. This appears to lead to impaired energy generation with a decline in [ATP] apparent early after treatment with the drug. Whereas this would normally lead to recruitment of AMPK, we find that AMPK is a direct target of sunitinib. This inhibits recruitment of some of the energy-conserving compensatory mechanisms that are ordinarily triggered by AMPK, as exemplified by impaired phosphorylation of ACC. Although the precise sequence



of events leading to mitochondrial injury is not clear and is probably multifactorial, the inability to recruit AMPK is critical, since cell death can be significantly reduced by expression of a constitutively active AMPK mutant. The striking improvement at the ultrastructural level with withdrawal of drug and institution of standard heart failure therapy suggests potential reversibility of sunitinib cardiotoxicity, though long-term follow-up of large numbers of patients will be required to assess this.

Sunitinib has shown efficacy in multiple types of solid tumors.<sup>1-3</sup> It is a multitargeted TKI in that it addresses both tumor cell proliferation and tumor angiogenesis, taking advantage of the fact that cancer cell proliferation and neoangiogenesis, which is required to support tumor growth,<sup>10,30,31</sup> are often driven by mutations in tyrosine kinases.<sup>32</sup> Although sunitinib makes logical sense from a cancer therapeutic standpoint, the targeting of multiple kinases by one drug leads to an inherent lack of selectivity, increasing the risk of off-target toxicities due to inhibition of additional kinases, the identity of which may or

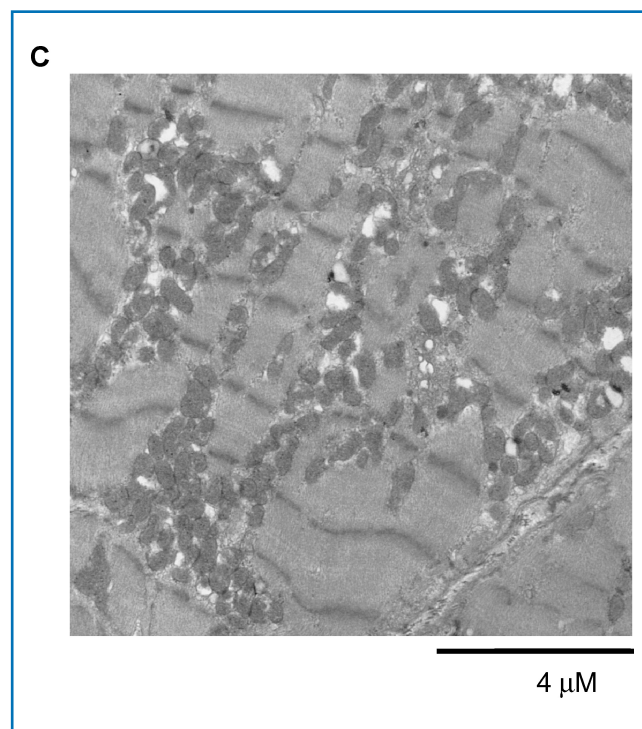


**Figure 6. Restoration of AMPK signaling rescues sunitinib-induced cell death.** (A) Restoration of AMPK signaling following adenoviral gene transfer of AMPK $\alpha$ -1(1-312). NRVMs were transduced with an adenovirus encoding AMPK $\alpha$ -1(1-312)(Ad.AMPK) versus GFP control (Ad.GFP) for 24 hours. Lysates were immunoblotted with the anti-phospho T172 AMPK antibody. Phosphorylation of endogenous AMPK (p-AMPK) and AMPK $\alpha$ -1(1-312)(V2 pAMPK) are shown. Bottom panel. Cells transduced as above were treated with 1  $\mu$ M sunitinib (+) or vehicle (-) for 8 hours, and lysates were immunoblotted for phospho-ACC.  $n = 4$ ;  $p < 0.01$ . (B) Reduction of sunitinib-induced cell death following gene transfer of AMPK $\alpha$ -1(1-312). NRVMs were transduced with adenovirus encoding either GFP or AMPK $\alpha$ -1(1-312) (Ad-AMPK V2) for 24 hours prior to being treated with 1  $\mu$ M sunitinib (+) or vehicle (-) for 28 hours. Cells were then stained for TUNEL and percent TUNEL positive cells was determined. (C) TEM of a follow-up endomyocardial biopsy from the patient shown in Figure 1. Image shows marked resolution of the pattern of mitochondrial abnormalities.

may not be known.<sup>33</sup> Our motivation to identify the key target(s) of sunitinib, inhibition of which led to cardiotoxicity, was based on earlier work by Fernandez et al., who demonstrated that if one could identify the TKI target, inhibition of which leads to toxicity, it is possible to redesign the TKI to no longer inhibit that target, reducing cardiotoxicity.<sup>6</sup>

The mitochondrial abnormalities clearly suggested that energy generation was impaired, and we confirmed this in cardiomyocytes in culture. AMPK is a critical kinase in times of energy depletion when ATP levels decline and AMP levels increase. Activation blocks energy consuming pathways, including protein translation/synthesis and fatty acid synthesis. AMPK also activates energy generating pathways by increasing fatty acid oxidation (via inhibition of ACC2) and glycolysis (via activation of phospho-fructo-2-kinase;<sup>17</sup> Figure 7A). Thus sunitinib-mediated inhibition of AMPK could release these energy-consuming pathways and prevent activation of energy generating pathways, exacerbating the energy rundown in the cell. Interestingly, regulation of the mTOR  $\rightarrow$  eEF2K  $\rightarrow$  eEF2 pathway seemed intact, likely reflecting the multiple inputs capable of regulating mTORC1 activity in the setting of energy compromise (Figure 7B).<sup>26</sup>



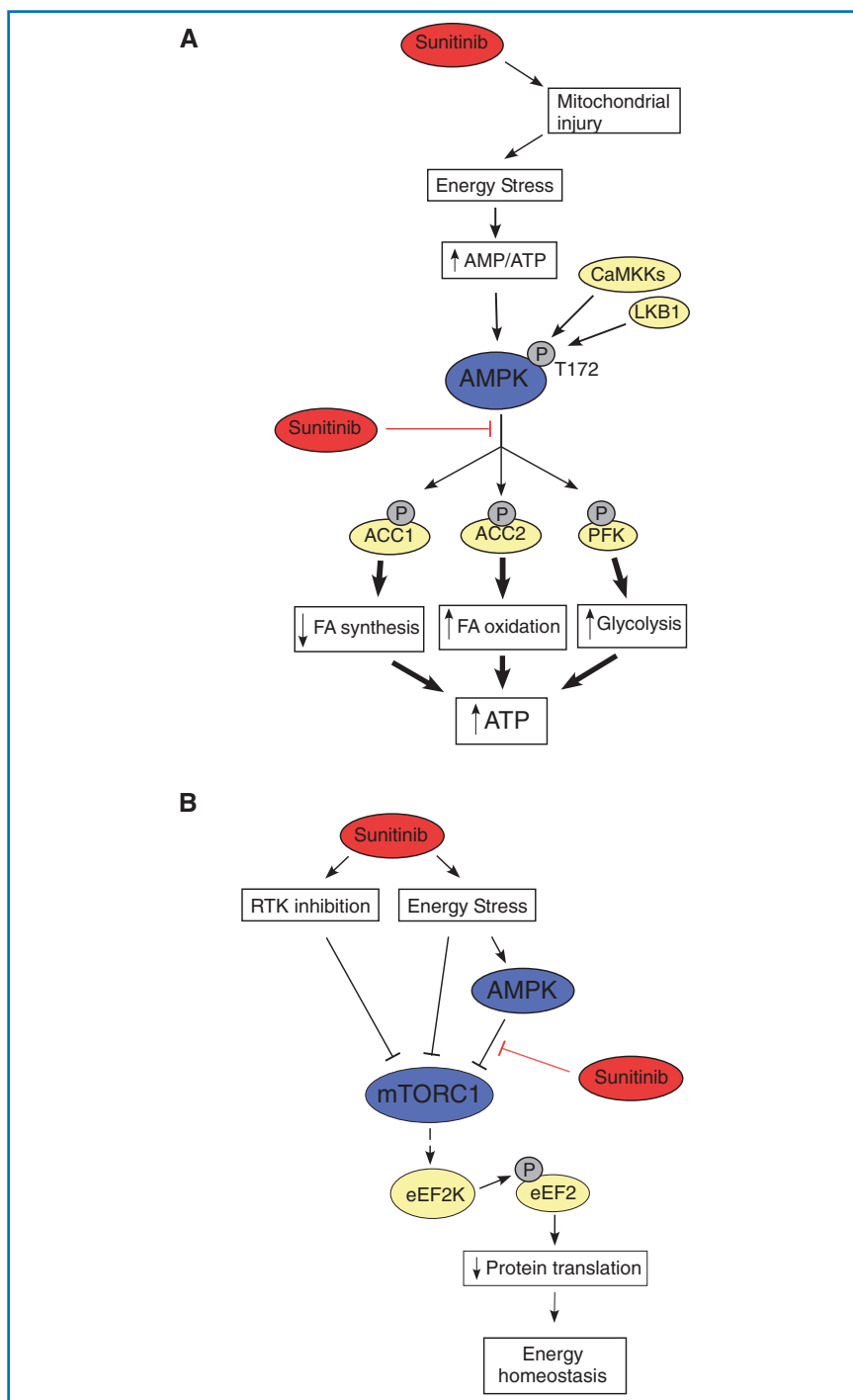


**Figure 7. Effects of sunitinib on energy-responsive signaling pathways in the heart. (A)** Inhibition of AMPK signaling by sunitinib. Energy stress (increase in AMP/ATP ratio), together with CaMKK- and/or LKB1-mediated phosphorylation of T172, lead to activation of AMPK. This produces a number of relatively rapid responses (phosphorylation of ACC1, ACC2, and phospho-fructokinase (PFK)), which lead to decreased fatty acid synthesis (ACC1), increased fatty acid oxidation (ACC2), and increased glycolysis (PFK). Longer-term responses include initiation of mitochondrial biogenesis via activation of PGC-1 $\alpha$  (not shown). Together, these responses help to restore energy homeostasis. However, in the presence of sunitinib, ATP cannot bind to AMPK, and therefore AMPK cannot transfer phosphate from ATP to the substrates. Thus, the energy conserving mechanisms are not recruited and energy depletion is exacerbated. **(B)** Effects of sunitinib on mTORC1 signaling and protein translation. Protein translation is a major energy consuming process in cardiomyocytes. AMPK activation by energy stress would normally inhibit mTORC1 signaling leading to increased eEF2 phosphorylation (mediated by eEF2Kinase), thereby inhibiting eEF2 activity. This leads to decreased protein translation and protein synthesis, thereby restoring energy homeostasis. In the presence of sunitinib, this mechanism is not active. However, multiple other AMPK-independent inputs, most notably inhibition of receptor tyrosine kinase (RTK) signaling and AMPK-independent mechanisms by which energy stress acts, can lead to inhibition of mTORC1, thereby inhibiting protein translation. Red lines indicate inhibitory inputs due to sunitinib.

That dysregulation of AMPK signaling secondary to sunitinib-mediated inhibition is critical is suggested by our findings demonstrating significant “rescue” of cell death following gene transfer of active AMPK. Thus, it seems clear that AMPK inhibition is necessary for the full expression of the cardiomyocyte toxicity. However, it is unclear whether AMPK inhibition alone is sufficient. Given the central role of AMPK in driving mitochondrial biogenesis and mitochondrial function,<sup>34,35</sup> it is possible that inhibition of AMPK in actively respiring cardiomyocytes may be sufficient to compromise energy status. While our data employing Compound C, which recapitulate most of the abnormalities seen with sunitinib, suggest that AMPK inhibition is sufficient, Compound C is not a selective inhibitor of AMPK. Thus, while it is unclear whether inhibition of AMPK is the initiating step leading to toxicity, it is clearly an important step. Of note, Will et al. recently reported that sunitinib is not directly toxic to mitochondria.<sup>36</sup>

Determining whether off-target inhibition of a kinase by a drug could be a mechanism of cardiotoxicity in patients is critically dependent on the dose employed in the experimental models (i.e., cultured cardiomyocytes and mice). If an excessive dose is used, findings concerning toxicity in those models may be irrelevant to the clinical situation. Our dosing regimen in mice was determined based on extensive pharmacokinetic data derived from preclinical studies of sunitinib.<sup>15,21,37</sup> We used 25 mg/kg/day in our studies *in vivo*, which is less than the 40 mg/kg/day dose in mice that produces blood levels similar to those seen in patients, yet saw significant inhibition of AMPK as evidenced by reduced phosphorylation of ACC. Thus sunitinib does inhibit AMPK in hearts of mice, at doses relevant to the clinical situation, and we believe that sunitinib likely does as well in the hearts of patients who receive the FDA-approved dose. However, the choice of a concentration to use in studies in cultured cells is more arbitrary, since although extensive *in vivo* pharmacokinetic data are available, it is difficult to translate that information into a precise concentration to use in cells in the absence of data on tissue levels achieved in the heart. Having said that, the trough blood levels and volume of distribution noted above suggest that our choice of a concentration of 0.5–1  $\mu$ M for these studies seems reasonable, and of note, this is one-fifth of the dose employed in Osusky et al.<sup>15,19,22,23</sup>

Recently Hasinoff et al.<sup>38</sup> reported that although AMPK was a target of sunitinib, AMPK inhibition was not an important mechanism of sunitinib cardiotoxicity. They based this conclusion on studies employing metformin, which can activate AMPK. In these studies, metformin failed to reduce sunitinib injury in NRVMs. We had tried a similar approach (i.e., pretreating cells with AICAR and then exposing them to sunitinib), and this also failed to rescue. However, we also found that in contrast to gene transfer of activated AMPK, which increased AMPK signaling even in the presence of sunitinib (Figure 6A, middle panel), AICAR failed to increase AMPK signaling in the setting of sunitinib (Figure 4D). Hasinoff et al. did not examine whether metformin was able to overcome sunitinib-mediated inhibition of AMPK, and we believe that this may account for the different conclusions reached in the two studies. Alternatively, the cell death assays reported in Hasinoff et al. employed very short-term treatment with sunitinib (3 hours) versus the 28 hours we employed, and this may also account in part for the differences.

In summary, we believe that we have identified a key mechanism contributing to the cardiotoxicity of sunitinib: off-target inhibition of AMPK. Our findings suggest that modification of sunitinib to no longer target AMPK might reduce cardiotoxicity. However, other data suggest that inhibition of AMPK in hypoxic cancer cells might be a key mechanism leading to tumor cell death.<sup>39,40</sup> If so, redesign of sunitinib or other agents to avoid AMPK inhibition is not feasible. Given the number of kinases that play prosurvival roles in both cancer cells and cardiomyocytes, coexisting cancer efficacy and cardiotoxicity will likely be a recurring theme. This highlights the critical importance of developing strategies to prevent and treat LV dysfunction in these patients.

## Acknowledgments

The authors thank Dr. Zhijun Luo for the kind gift of the adenovirus encoding the constitutively active AMPK mutant, AMPK $\alpha$ -1(1–312) and Dr. Walter Kraft for helpful discussions. The authors are deeply indebted to Dr. James Christensen and Pfizer, Inc. for providing the results of the kinase inhibitor studies. This work was supported by grants from the NHLBI: RO1 HL061688 and PO1 HL091799 (to TF), the Finnish Heart Foundation and Finnish Cultural Foundation (to R. K.), the American Heart Association (to K. C. W.), and the Translational Fund for Cardiology and Oncology of Children's Hospital Boston (to M. H. C.).

## References

- Demetri GD, van Oosterom AT, Garrett CR, Blackstein ME, Shah MH, Verweij J, McArthur G, Judson IR, Heinrich MC, Morgan JA, Desai J, Fletcher CD, George S, Bello CL, Huang X, Baum CM, Casali PG. Efficacy and safety of sunitinib in patients with advanced gastrointestinal stromal tumour after failure of imatinib: A randomised controlled trial. *Lancet*. 2006; 368: 1329–1338.
- Motzer RJ, Hutson TE, Tomczak P, Michaelson MD, Bukowski RM, Rixe O, Oudard S, Negrier S, Szczylik C, Kim ST, Chen I, Bycott PW, Baum CM, Figlin RA. Sunitinib versus interferon alfa in metastatic renal-cell carcinoma. *N Engl J Med*. 2007; 356: 115–124.
- Favre S, Demetri G, Sargent W, Raymond E. Molecular basis for sunitinib efficacy and future clinical development. *Nat Rev Drug Discov*. 2007; 6: 734–745.
- Chu T, Rupnick MA, Kerkela R, Dallabrida SM, Zurakowski D, Nguyen L, Woulfe K, Pravda E, Cassiola F, Desai J, George S, Morgan JA, Harris DM, Ismail NS, Chen J-H, Schoen FJ, Demetri GD, Force T, Chen MH. Cardiotoxicity associated with the tyrosine kinase inhibitor sunitinib. *Lancet*. 2007; 270: 2011–2019.
- Telli ML, Witteles RM, Fisher GA, Srinivas S. Cardiotoxicity associated with the cancer therapeutic agent sunitinib malate. *Ann Oncol*. 2008; 19: 1613–1618.

- Fernandez A, Sanguino A, Peng Z, Ozturk E, Chen J, Crespo A, Wulf S, Shavrin A, Qin C, Ma J, Trent J, Lin Y, Han H-D, Mangala LS, Bankson JA, Gelovani J, Samarel A, Bornmann W, Sood AK, Lopez-Bernstein G. An anticancer c-Kit kinase inhibitor is reengineered to make it more active and less cardiotoxic. *J Clin Invest*. 2007; 117: 4044–4054.
- Kerkela R, Grazette L, Yacobi R, Iliescu C, Patten R, Beahm C, Walters B, Shevtsov S, Pesant S, Clubb FJ, Rosenzweig A, Salomon RN, Van Etten RA, Alroy J, Durand JB, Force T. Cardiotoxicity of the cancer therapeutic agent imatinib mesylate. *Nat Med*. 2006; 12: 908–916.
- Force T, Krause DS, Van Etten RA. Molecular mechanisms of cardiotoxicity of tyrosine kinase inhibition. *Nat Rev Cancer*. 2007; 7: 332–344.
- Verheul HMW, Pinedo HM. Possible molecular mechanisms involved in the toxicity of angiogenesis inhibition. *Nat Rev Cancer*. 2007; 7: 475–485.
- Chen MH, Kerkela R, Force T. Mechanisms of cardiac dysfunction associated with tyrosine kinase inhibitor cancer therapeutics. *Circulation*. 2008; 118: 84–95.
- Shiojima I, Sato K, Izumiya Y, Schiekofer S, Ito M, Liao R, Colucci WS, Walsh K. Disruption of coordinated cardiac hypertrophy and angiogenesis contributes to the transition to heart failure. *J Clin Invest*. 2005; 115: 2108–2118.
- Edelberg JM, Lee SH, Kaur M, Tang L, Feirt NM, McCabe S, Bramwell O, Wong SC, Hong MK. Platelet-derived growth factor-AB limits the extent of myocardial infarction in a rat model: Feasibility of restoring impaired angiogenic capacity in the aging heart. *Circulation*. 2002; 105: 608–613.
- Hsieh PC, MacGillivray C, Gannon J, Cruz FU, Lee RT. Local controlled intramyocardial delivery of platelet-derived growth factor improves postinfarction ventricular function without pulmonary toxicity. *Circulation*. 2006; 114: 637–644.
- Chen X, Shevtsov S, Hsieh E, Cui L, Haq S, Aronovitz MJ, Kerkela R, Molkentin JD, Liao R, Salomon R, Patten RD, Force T. The  $\beta$ -catenin/T-cell factor/Lymphocyte enhancer factor signaling pathway is required for normal and stress-induced cardiac hypertrophy. *Mol Cell Biol*. 2006; 26: 4462–4473.
- Osusky KL, Hallahan DE, Fu A, Ye F, Shyr Y, Geng L. The receptor tyrosine kinase inhibitor SU11248 impedes endothelial cell migration, tubule formation, and blood vessel formation in vivo, but has little effect on existing tumor vessels. *Angiogenesis*. 2004; 7: 225–233.
- Arad M, Seidman CE, Seidman JG. AMP-activated protein kinase in the heart: Role during health and disease. *Circ Res*. 2007; 100: 474–488.
- Towler MC, Hardie DG. AMP-activated protein kinase in metabolic control and insulin signaling. *Circ Res*. 2007; 100: 328–341.
- Young LH, Li J, Baron SJ, Russell RR. AMP-activated protein kinase: A key stress signaling pathway in the heart. *Trends Cardiovasc Med*. 2005; 15: 110–118.
- Kim DW, Jo YS, Jung HS, Chung HK, Song JH, Park KC, Park SH, Hwang JH, Rha SY, Kweon GR, Lee SJ, Jo KW, Shong M. An orally administered multitarget tyrosine kinase inhibitor, SU11248, is a novel potent inhibitor of thyroid oncogenic RET/papillary thyroid cancer kinases. *J Clin Endocrinol Metab*. 2006; 91: 4070–4076.
- Favre S, Delbaldo C, Vera K, Robert C, Lozahic S, Lassau N, Bello C, Deprimo S, Brega N, Massimini G, Armand JP, Scigalla P, Raymond E. Safety, pharmacokinetic, and antitumor activity of SU11248, a novel oral multitarget tyrosine kinase inhibitor, in patients with cancer. *J Clin Oncol*. 2006; 24: 25–35.
- Mendel DB, Laird AD, Xin X, Louie SG, Christensen JG, Li G, Schreck RE, Abrams YJ, Ngai TJ, Lee LB, Murray LJ, Carver J, Chan ED, Moss KG, Haznedar JO, Sukbunthorn J, Blake RA, Sun L, Tang C, Miller TA, Shirazian S, McMahon G, Cherrington JM. In vivo antitumor activity of SU11248, a novel tyrosine kinase inhibitor targeting vascular endothelial growth factor and platelet-derived growth factor receptors: Determination of a pharmacokinetic/pharmacodynamic relationship. *Clin Cancer Res*. 2003; 9: 327–337.
- Fiedler W, Serve H, Dohner H, Schwittay M, Ottmann OG, O'Farrell AM, Bello CL, Allred R, Manning WC, Cherrington JM, Louie SG, Hong W, Brega NM, Massimini G, Scigalla P, Berdel WE, Hossfeld DK. A phase 1 study of SU11248 in the treatment of patients with refractory or resistant acute myeloid leukemia (AML) or not amenable to conventional therapy for the disease. *Blood*. 2005; 105: 986–993.
- Roskoski R, Jr. Sunitinib: a VEGF and PDGF receptor protein kinase and angiogenesis inhibitor. *Biochem Biophys Res Commun*. 2007; 356(2): 323–328.
- Dyck JR, Lopaschuk GD. AMPK alterations in cardiac physiology and pathology: Enemy or ally? *J Physiol*. 2006; 574: 95–112.
- Wang X, Proud CG. The mTOR pathway in the control of protein synthesis. *Physiology (Bethesda, Md)*. 2006; 21: 362–369.
- Huang J, Manning BD. The TSC1-TSC2 complex: A molecular switchboard controlling cell growth. *Biochem J*. 2008; 412: 179–190.
- Arsham AM, Howell JJ, Simon MC. A novel hypoxia-inducible factor-independent hypoxic response regulating mammalian target of rapamycin and its targets. *J Biol Chem*. 2003; 278: 29655–29660.
- Brugarolas J, Lei K, Hurlley RL, Manning BD, Reiling JH, Hafen E, Witters LA, Ellisen LW, Kaelin WG, Jr. Regulation of mTOR function in response to hypoxia by REDD1 and the TSC1/TSC2 tumor suppressor complex. *Genes Dev*. 2004; 18: 2893–2904.
- Fabian MA, Biggs WH, Treiber DK, Atteridge CE, Azimioara MD, Benedetti MG, Carter TA, Ciceri P, Edeen PT, Floyd M, Ford JM, Galvin M, Gerlach JL, Grotzfeld RM, Herrgard S, Insko DE, Insko MA, Lai AG, Lelias JM, Mehta SA, Milanov ZV, Velasco AM, Wodicka LM, Patel HK, Zarrinkar PP, Lockhart DJ. A small molecule-kinase interaction map for clinical kinase inhibitors. *Nat Biotechnol*. 2005; 23: 329–336.

30. Folkman J. Angiogenesis: An organizing principle for drug discovery? *Nat Rev Drug Discov.* 2007; 6: 273–286.
31. Jain RK, Duda DG, Clark JW, Loeffler JS. Lessons from phase III clinical trials on anti-VEGF therapy for cancer. *Nat Clin Pract Oncol.* 2005; 3: 24–40.
32. Krause DS, Van Etten RA. Tyrosine kinases as targets for cancer therapy. *N Engl J Med.* 2005; 353: 172–187.
33. Bantscheff M, Eberhard D, Abraham Y, Bastuck S, Boesche M, Hobson S, Mathieson T, Perrin J, Rida M, Rau C, Reader V, Sweetman G, Bauer A, Bouwmeester T, Hopf C, Kruse U, Neubauer G, Ramsden N, Rick J, Kuster B, Drewes G. Quantitative chemical proteomics reveals mechanisms of action of clinical ABL kinase inhibitors. *Nat Biotechnol.* 2007; 25: 1035–1044.
34. Finck BN, Kelly DP. Peroxisome proliferator-activated receptor gamma coactivator-1 (PGC-1) regulatory cascade in cardiac physiology and disease. *Circulation.* 2007; 115: 2540–2548.
35. Zong H, Ren JM, Young LH, Pypaert M, Mu J, Birnbaum MJ, Shulman GI. AMP kinase is required for mitochondrial biogenesis in skeletal muscle in response to chronic energy deprivation. *Proc Natl Acad Sci USA.* 2002; 99: 15983–15987.
36. Will Y, Dykens JA, Nadanaciva S, Hirakawa B, Jamieson J, Marroquin LD, Hynes J, Patyna S, Jessen BA. Effect of the multi-targeted tyrosine kinase inhibitors imatinib, dasatinib, sunitinib and sorafenib on mitochondrial function in isolated rat heart mitochondria and H9c2 cells. *Toxicol Sci.* 2008; 106: 153–161.
37. Schueneman AJ, Himmelfarb E, Geng L, Tan J, Donnelly E, Mendel D, McMahon G, Hallahan DE. SU11248 maintenance therapy prevents tumor regrowth after fractionated irradiation of murine tumor models. *Cancer Res.* 2003; 63: 4009–4016.
38. Hasinoff BB, Patel D, O'Hara KA. Mechanisms of myocyte cytotoxicity induced by the multiple receptor tyrosine kinase inhibitor sunitinib. *Mol Pharm.* 2008; 74: 1722–1728.
39. Liu L, Cash TP, Jones RG, Keith B, Thompson CB, Simon MC. Hypoxia-induced energy stress regulates mRNA translation and cell growth. *Mol Cell.* 2006; 21: 521–531.
40. Luo Z, Saha AK, Xiang X, Ruderman NB. AMPK, the metabolic syndrome and cancer. *Trends Pharmacol. Sci.* 2005; 26: 69–76.

## Supporting Information

The following supporting information is available for this article:

**Figure S1.** Top panel. NRVMs were pretreated with vehicle (sunitinib 0  $\mu\text{M}$ ) or sunitinib (1  $\mu\text{M}$ ) for 4 hours. Cells were then treated with the AMPK activator, AICAR (1 mM) versus vehicle (–) for 1 hour. Lysates were immunoblotted with an antibody to total ACC. Quantification of expression levels of ACC normalized to vinculin are shown below the immunoblot. Bottom panel. NRVMs were treated with sunitinib (1  $\mu\text{M}$ ) for the times shown, and then lysates were immunoblotted for total AMPK. AMPK expression, normalized to GAPDH, is shown below the immunoblot.

**Figure S2.** NRVMs were transduced with an adenovirus encoding AMPK $\alpha$ -1(1–312) (Ad.AMPK) or control virus encoding GFP (Ad.GFP) exactly as described in the legend of Figure 6A. Lysates were then immunoblotted with an antibody recognizing AMPK.

Please note: Wiley-Blackwell Publishing is not responsible for the content or functionality of any supporting information supplied by the authors. Any queries (other than missing material) should be directed to the corresponding author for the article.

This material is available as part of the online article from <http://www.ctsjournal.com>.